Materials Advances

ROYAL SOCIETY OF CHEMISTRY

PAPER

View Article Online
View Journal | View Issue



Cite this: *Mater. Adv.*, 2024, 5, 8164

# Facile fabrication of stretchable, anti-freezing, and stable organohydrogels for strain sensing at subzero temperatures†

Muhammad Sher,[a] Luqman Ali Shah,*[a] Jun Fu,[b] Hyeong-Min Yoo,[c] Riaz Ullah[d] and Mohamed A. Ibrahim[e]

Conductive hydrogel-based soft devices are gaining increasing attention. Still, their dependence on water makes them susceptible to freezing and drying, which affects their long-term stability and durability and limits their applications under subzero temperatures. Developing hydrogels that combine exceptional strength, high strain sensitivity, anti-freezing properties, synchronous sensing, durability, and actuating capabilities remains a significant challenge. To overcome these issues, a universal solvent replacement strategy (USRS) was adopted to fabricate anti-freezing and anti-drying organohydrogels with ultra stretchability and high strain sensitivity in a wide temperature range. Ethylene glycol (Eg) and glycerol (Gl) were used as secondary solvents to replace water (primary solvent) from the hydrogel network. Due to the strong hydrogen bonding capabilities of Eg and Gl with water and the hydrogel network, the organohydrogels formed show resistance to freezing and drying. This allows the organohydrogels to maintain conductivity, sensitivity, stretchability, and durability under subzero temperatures. The developed organohydrogels display remarkable stretchability (850%), good electrical conductivity (0.45 S $m^{-1}$), exceptional anti-freezing performance below −90 °C and very high sensitivity (GF = 10.14). Additionally, the strain sensor demonstrates a notably wide strain range (1–600%) checked within the temperature range of −15 °C to 25 °C. It also effectively monitors various human movements with differing strain levels, maintaining good stability and repeatability from −15 to 25 °C. It is also believed that this strain sensor can work efficiently above and below the mentioned temperature range. This study introduced a straightforward approach to developing conductive organohydrogels with outstanding anti-freezing and mechanical properties, demonstrating significant potential for use in wearable strain sensors and soft robotics.

Received 17th July 2024,
Accepted 14th September 2024

DOI: 10.1039/d4ma00725e

rsc.li/materials-advances



## 1. Introduction

The demand for stretchable and flexible electronic devices is increasing daily due to potential applications in various fields. The need for electronic skin (e-skin), touch panels, stretchable electrodes, soft robotics, and prosthetics is gaining interest from future generations.[1–3] Conventional rigid robots often struggle in environments with unpredictable terrain, extreme temperatures, or the presence of delicate objects. Apart from these, rigid robots have certain other limitations like limited mobility and stretchability, complicated fabrication procedures, susceptibility to damage, and heavy and large size issues.[4,5] Additionally, rigid robots suffer from complexity in modeling, sensing, and control systems, which are of particular interest to the robotics community.[6]

Soft robotics is an emerging field that involves the design and development of robots. Strain sensing is a vital feature of soft robots, allowing them to establish a tactile interface resembling human skin when interacting with their surroundings. To meet soft robot compliance and morphology needs, sensing materials must possess softness and stretchability to minimize interference with the robot movements.[7] Traditional practice involves engineering nano-materials like low-dimensional

[a] *Polymer Laboratory, National Centre of Excellence in Physical Chemistry, University of Peshawar, 25120, Pakistan. E-mail: luqman_alisha@uop.edu.pk, Luqman_alisha@yahoo.com; Fax: +92-91-9216671; Tel: +92-91-9216766*
[b] *Key Laboratory of Polymeric Composite and Functional Materials, School of Materials Science and Engineering, Sun Yat-sen University, Guangzhou 510275, China*
[c] *School of Mechanical Engineering, Korea University of Technology and Education (KOREATECH), Cheonan 31253, Republic of Korea*
[d] *Department of Pharmacognosy, College of Pharmacy, King Saud University, Riyadh, Saudi Arabia*
[e] *Department of Pharmaceutics, College of Pharmacy, King Saud University, Riyadh 11451, Saudi Arabia*

† Electronic supplementary information (ESI) available. See DOI: https://doi.org/10.1039/d4ma00725e

carbon materials, metal nanowires, and silicon nano-ribbons on elastic substrates to create stretchable strain sensors for robot incorporation, but they usually suffer from low mechanical performance.[7]

This issue has been resolved using intrinsically stretchable materials that offer a straightforward solution, boasting simple fabrication processes, affordability, strong mechanical resilience, and a high device density.[8] In this regard, hydrogels, three-dimensional (3D) polymeric networks, can hold substantial amounts of water without leaking primarily due to their 3D structure. This feature equips them with advantageous properties akin to living tissues, making them highly valuable for diverse applications in biomedicine and soft electronics.[9,10]

In the past decade, scientists have greatly improved the weak areas of hydrogels. For example, various approaches have been investigated to tackle the issue of weak mechanical properties. These include the development of double-network structures, enhancing crosslinking density, employing multi-functional crosslinkers, and introducing an anisotropic configuration. In particular, double-networked (DN) hydrogels, comprising a rigid network and a ductile matrix, demonstrate improved mechanical strength, resilience, and functional attributes compared to their single-networked counterparts.

Recent reports have also showcased hydrogel-based strain and pressure sensors that boast exceptional stretchability. For example, Yazdani *et al.* developed a robust hydrogel by combining lauryl methacrylate, acrylamide, and sodium alginate through a cross-linked network for ionic skin and human motion detection.[11] Ullah *et al.* have developed a mechanically strong hydrogel with fracture stress and strain that reached 0.5 MPa and 401%, respectively, having gauge factor values 8.2.[12] Similarly, in our previous work, we developed hydrogels for flexible and artificial epidermis with an enhanced mechanical performance of 1100% and a fracture strain of 661 kPa with high sensitivity having a gauge factor value of 28.8.[9] However, hydrogels unavoidably solidify below-freezing temperatures, resulting in stiffness, fragility, and loss of conductivity.[13,14] Furthermore, these strategies need to be revised to control excess water, leading to environmentally unstable hydrogels that frequently need to meet the criteria for long-term durability. Hence, the utilization of hydrogel-based devices is impeded in low-temperature environments. Even under room temperature or higher, hydrogels inevitably experience dehydration through water evaporation.[15,16] The inherent problems of freezing and drying lead to loss in flexibility, stretchability, conductivity, and other properties in water-based hydrogels, significantly undermining their stability and durability, and the potential applications of devices they are used in.[17,18]

Eg and Gl, well-known humectant and anti-freezing agents used in industry, have high boiling points and low volatility at room temperature compared to water. Replacing water with ethylene glycol and glycerol endowed the hydrogels with enhanced durability, anti-drying, and anti-freezing properties.[19,20] They prevent water from freezing by creating strong hydrogen bonds with water molecules while simultaneously breaking the hydrogen bonds between water molecules.[8,13] Notably, by adjusting the Eg and Gl concentration in the organohydrogels, the freezing point can be lowered to as much as −40 °C, significantly below the freezing points of pure Eg and water.[20,21]

Herein, we describe a straightforward USRS for creating strong, ultra-stretchable, and stable organohydrogels with conductive, anti-freezing, and anti-drying characteristics for soft robotics and human–machine interaction. Hexadecyltrimethylammonium bromide (HDAB) was dissolved in distilled water to produce a micelle structure in which hydrophobic monomer lauryl methacrylate (LM) stabilizes itself. Then, acrylamide (Am) and LM copolymer were grafted onto the agar (Ag) chain using ammonium persulphate (APS) as a thermal initiator. Incorporating Ag improves the hydrogel's mechanical characteristics and makes it more challenging. Moreover, the synthesized hydrogels were successfully converted into organohydrogels through USRS using different Eg and Gl concentrations in individual states and binary solution form. The obtained anti-freezing organohydrogels displayed enhanced stretchability (up to 850% strain), anti-drying, and strain-sensing capability at −15 °C. Thus, the strain sensors based on organohydrogels can be applied in soft robotics and human–machine interaction technologies with great stability, high sensitivity (GF = 10.14), wide strain range (1–600%), and a wide temperature range.

## 2. Experimental section

### 2.1. Materials

Acrylamide (Am) was purchased from BDH, lauryl methacrylate (LM) from Acros organics and cobalt chloride hexahydrate ($CoCl_2{\cdot}6H_2O$) from Scharlau, and hexadecyltrimethylammonium bromide (HDAB), agar (Ag), ammonium persulphate (APS), ethylene glycols (Eg), and glycerol (Gl) were purchased from Sigma-Aldrich. During the experiment, double distilled water (DW) was used and all of the chemicals used were of analytical grade.

### 2.2. Fabrication of poly(Am-*co*-LM@Ag) hydrogels

The hydrogels of poly(Am-*co*-LM@Ag) were synthesized by a facile one-pot free radical polymerization strategy as reported previously.[22,23] Specifically, 0.4 gram (g) of HDAB was added into 10 mL DW followed by 600 μL LM and stirred moderately for 10 minutes (min); after that, 2 g of Am and 0.3 g of $CoCl_2{\cdot}6H_2O$ was added. After stirring for 10 min, the solution was charged with 0.02 g of Ag and stirred at 700 revolutions per minute (rpm) for 3 hours (hrs) for fine solution formation. Finally, 0.05 g of APS was added to it and stirred for an additional 1 min. The solution was then transferred into a plastic mold having 70 mm length and 30 mm width and kept in an oven at 60 °C for 2.5 hrs.

### 2.3. Fabrication of organohydrogels

The organohydrogels were fabricated using USRS.[8] The as-fabricated poly(Am-*co*-LM@Agar) hydrogels were soaked in 100 wt% Eg, 100 wt% Gl, 50% Eg + 50% Gl, 30 wt% Eg + 70 wt% Gl, and 30 wt% Gl + 70 wt% Eg for 1 hr for the

generation of the corresponding organohydrogels. After the samples were removed from the solution, the extra solvent present on the surface of each sample was removed with filter paper. Similarly, for a comparative study a sample was synthesized without soaking in any of the mentioned solvents. We also synthesized a sample without adding Ag into it to better understand the functioning of Ag in the synthesized material.

### 2.4. Tests and characterization of the sensors

Different characterization tests were performed to investigate the as-fabricated organohydrogels. The organohydrogels were utilized as a channel material for creating strain sensors with a two-electrode configuration in an automated lab system. A rectangular piece of organohydrogel was attached between two electrodes connected to a potentiostat/galvanostat AUTOLAB (Modular Multi-Channel M204). Chronoamperometry was used to monitor the sensor conductance (current response) by applying a fixed potential of 1 V. The system current response was converted into resistance using Ohm's law ($V = IR$), followed by the calculation of percentage relative resistances (RRs) using eqn (1), as reported in the previous literature.[24,25]

$$\mathrm{RR}\ (\%) = \left(\frac{R - R_0}{R_0}\right) \times 100 \quad (1)$$

where $R_0$ is the initial resistance and $R$ is the final resistance.

To subject the sensor to desired strains during the electromechanical test, the ends of the samples were secured onto the two-electrode system using a stretching stage labeled carefully for each desired strain in increasing order.

The electromechanical properties of the organohydrogel sensors for low-temperature strain sensing were investigated immediately upon its removal from the −15 °C environment. After removing it from the subzero temperature, we performed only one test each time and stored it again for one hr. In this process, we alternatively used five samples of the same composition and equal dimensions. A similar configuration was utilized to study human motion monitoring, sensitivity (gauge factor), and pressure sensing.

Similarly, the viscoelastic properties of the designed hydrogels and organohydrogels were examined using an Anton Paar rheometer (Physica MCR 301) equipped with a 25 mm diameter measuring probe. Amplitude sweep tests were conducted over a strain range of 0.01 to 1000% at a constant frequency of 10 rad $s^{-1}$, while frequency sweep experiments covered frequencies from 0.1 to 100 rad $s^{-1}$; throughout the rheological analysis, the temperature was maintained at 25 °C. Percentage changes in storage modulus were calculated using eqn (2).[25]

$$\%\Delta X = \left(\frac{X_2 - X_1}{X_1}\right) \times 100 \quad (2)$$

hydrogels and organohydrogels of known dimensions (50 mm length, 10 mm width, and 1 mm thickness) were prepared for mechanical analysis. A universal testing machine (UTM) from Test Metric England, with a capacity of 30 kN, a 500 N load cell, and a test rate of 50 mm $min^{-1}$, was employed. The toughness ($U$) of the hydrogels was determined by calculating the area under the stress–strain curve. Likewise, the dissipation energy ($\Delta U$) was determined by computing the area enclosed between the cyclic loading and unloading curves.[26]

The conductivity of the organohydrogels was checked by using an LCR machine. A piece of known dimension organohydrogel was investigated for RS (series resistance) value by connecting it in the two electrodes of the device. The values were utilized to get the conductivity of the organohydrogels using eqn (3).[25]

$$\text{Conductivity} = \frac{L}{R \cdot A} \quad (3)$$

where $L$ is the length, $A$ is the cross-section area, and $R$ is the bulk resistance of the organohydrogels.

The water retention capability of the organohydrogels was validated through a comparative study with a hydrogel. In this study, samples S1, S2, S3, and S6 were kept at room temperature (RT) and pressure and relative humidity (RH) of 58% in an open environment. Over the course of two months, the water loss was monitored, and their water retention capabilities were ultimately compared.

Differential scanning calorimetry (DSC) curves of the samples were acquired using a DSC-204 F1 instrument from Netzsch, Germany in the temperature range of 25 to −90 °C.

## 3. Results and discussion

### 3.1. Synthesis of ultimate anti-freezing organohydrogels

A one-pot free radical polymerization approach was used to synthesize the hydrogels.[25,27] During the synthesis, Ag was used as a reinforcement agent to create physical cross-linking sites to achieve mechanically robust hydrogels. APS was employed as the thermal initiator in the polymerization process of poly(Am-*co*-LM@Ag). At the beginning of the experiment, HDAB was added to distilled water to produce micelle cores.[28] The hydrophobic monomer LM possesses a hydrophilic head and a long hydrophobic tail. The micelles work to stabilize the hydrophobic tail of LM by allowing it to move inside its core structure, whereas the hydrophilic region remains outside the core region of the micelles, as shown in Fig. S1 (ESI†). APS being a thermal initiator produces Am free radicals as well as LM free radicals after its activation at 60 °C. During the polymerization, the Am free radical combined with the LM free radical and underwent polymerization, which established a dynamic linkage through the micelles.

Similarly, the addition of Ag to the solution led to the formation of stable hydrogels due to its capability to form physical cross-linking (hydrogen bonding) with both LM and Am due to numerous numbers of active sites on its chain, as shown in Fig. S1 (ESI†) and reported in previous literature.[29] Furthermore, the stability can also be attributed to the capability of the Ag to link to the hydrogel structure from different sites. The addition of $CoCl_2{\cdot}6H_2O$ imparts conductivity to the hydrogels and makes it best fit for sensing applications.

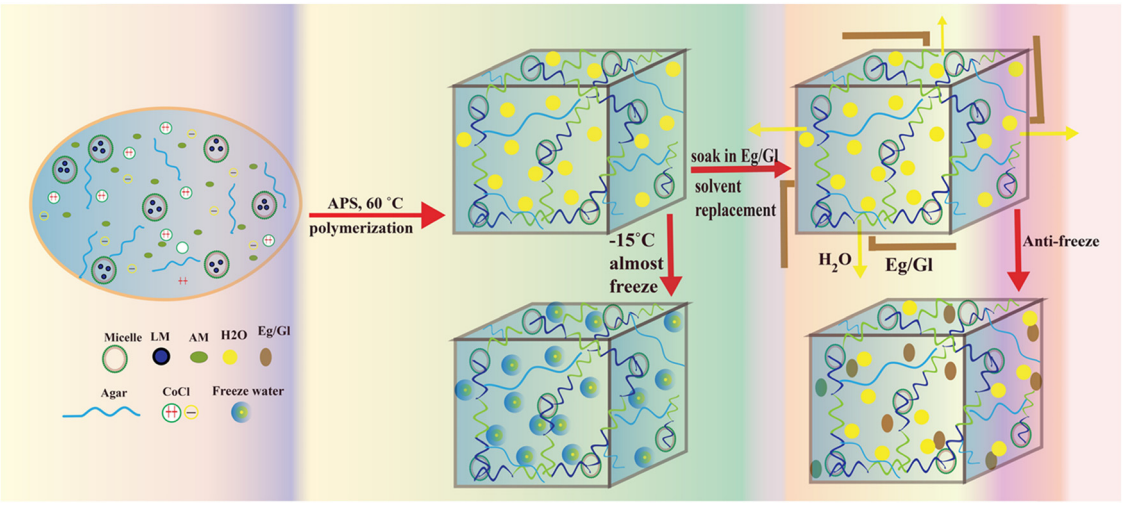


Fig. 1 Diagram showing the polymerization and subsequently simple USRS used to create anti-freezing DN organohydrogels from DN hydrogels. At −15 °C, the DN hydrogels solidified; however, the Eg and Gl anti-freezing organohydrogels retained their elasticity even at such low temperatures.

A sample without Ag was synthesized to investigate the effect of Ag on the hydrogels mechanical performance.

Similarly, the organohydrogels were prepared by following the USRS driven by the concentration difference, as shown in Fig. 1 and reported in previous literature.[8] The as-fabricated water-based hydrogels were directly immersed in an Eg and Gl solution to exchange water molecules from the hydrogel network with an outside Eg and Gl solution. Due to the difference in concentration, the molecular exchange occurred swiftly until reaching equilibrium. Consequently, the initial water-based hydrogels were transformed into organohydrogels using Eg and Gl in the individual states and a binary solvent, displaying enhanced capabilities to resist freezing and dehydration. To explore the impact of solvents on the anti-freezing properties of the product material, identical batches of hydrogels were submerged in five distinct solutions. These solutions comprised 100 wt% Eg, 100 wt% Gl, 50 wt% of Eg/Gl each, 30 wt% Eg + 70 wt% Gl, and 30 wt% Gl + 70 wt% Eg, for equal durations, yielding respective samples labeled S1 through S5. Similarly, a sample containing only water (not soaked) is named as S6, while a sample without Ag was prepared and coded as sample S0.

### 3.2. Analysis of anti-freezing behavior

To confirm the anti-freezing behavior of the as-synthesized organohydrogels, samples S1, S2, and S6 were kept at −15 °C for 2 hours. As shown in Fig. 2, the original hydrogels labeled as S6 froze up and cannot bear strain greater than 350%. The frozen state can be identified through the naked eye due to the pinky-white and opaque color formation. At the same time, samples S1 and S2 resist freezing and can be stretched to 9 times their initial length, and withstand 750% and 850% applied percent strain at −15 °C or even more than that (recorded here is 850%), respectively, as shown in Video S1 (ESI†).

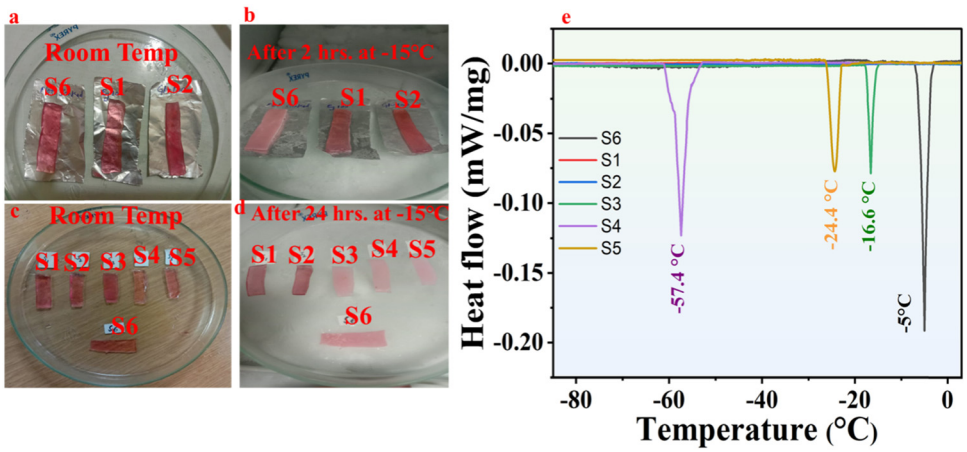


Fig. 2 Photographs showing anti-freezing characteristics of the hydrogels and organohydrogels at −15 °C. (a) Room temperature photographs of samples S1, S2 and S6, (b) S1, S2 and S3 after storing for two hours at −15 °C, (c) S1–S6 at room temperature and (d) S1–S6 after storing for 24 hours at −15 °C. (e) DSC curves.

The samples from S1–S6 were kept at −15 °C for 24 hours. It was observed that the sample soaked in pure Gl and pure Eg could withstand stretching performance approximately to the same level of applied percent strain as discussed above.

Conversely, all the other samples had almost frozen up after 24 hours of treatment and could not withstand such large deformations. This suggests the importance of Eg and Gl solvent and its efficiency in imparting anti-freezing characteristics in the organohydrogels reported in previous literature.[30] It has also been clear that the lowest freezing point of the organohydrogels is obtained when the hydrogel was dipped in 100% Eg and 100% Gl for 1 hour.[8] By contrast, hydrogels dipped in low concentrations of Eg and Gl solution could not achieve the required amount of solvent replacement. The competition between the solvents, combined with their diluted effective concentrations, reduces their ability to efficiently penetrate the hydrogel matrix and replace the internal water content, leading to incomplete solvent replacement. Furthermore, the incomplete swelling dynamics results in only a small amount of solvent replacement leaving the hydrogel matrix less modified than intended. Hence, samples S1 and S2 demonstrate superior anti-freezing capacity compared to S3, S4, and S5. Fig. S2 (ESI†) presents images comparing the stretching performance of the hydrogels and organohydrogels at room temperature and after storing at −15 °C for two hours. It is clear from the images in Fig. S2(A, a) (ESI†) that the stretching ability of the hydrogels has decreased after keeping at subzero temperature; conversely, the stretching performance of samples S1 and S2 is not as such affected by storing at subzero temperature (Fig. S2(B, b and C, c), ESI†). These samples can maintain their ability to stretch at various strains even after being stored at −15 °C for 24 hours, showcasing remarkable resilience under subzero conditions. While our current experimental setup registers −15 °C as the minimum temperature, there's a possibility that the organohydrogels could resist freezing even at lower temperatures. Therefore, employing the solvent replacement strategy offers a convenient avenue for adjusting the freezing resilience of organohydrogels by manipulating the concentration of antifreeze agents. The significantly enhanced anti-freezing capability observed in the resulting organohydrogels also suggests successful modification of Eg and Gl within the hydrogels through the USRS. Moreover, we conducted a thorough examination of the anti-freezing characteristics of the hydrogels and organohydrogels by analyzing the DSC curves of the samples, as shown in Fig. 2e. The analysis revealed a broad and long crystallization peak for samples S4 and S6.

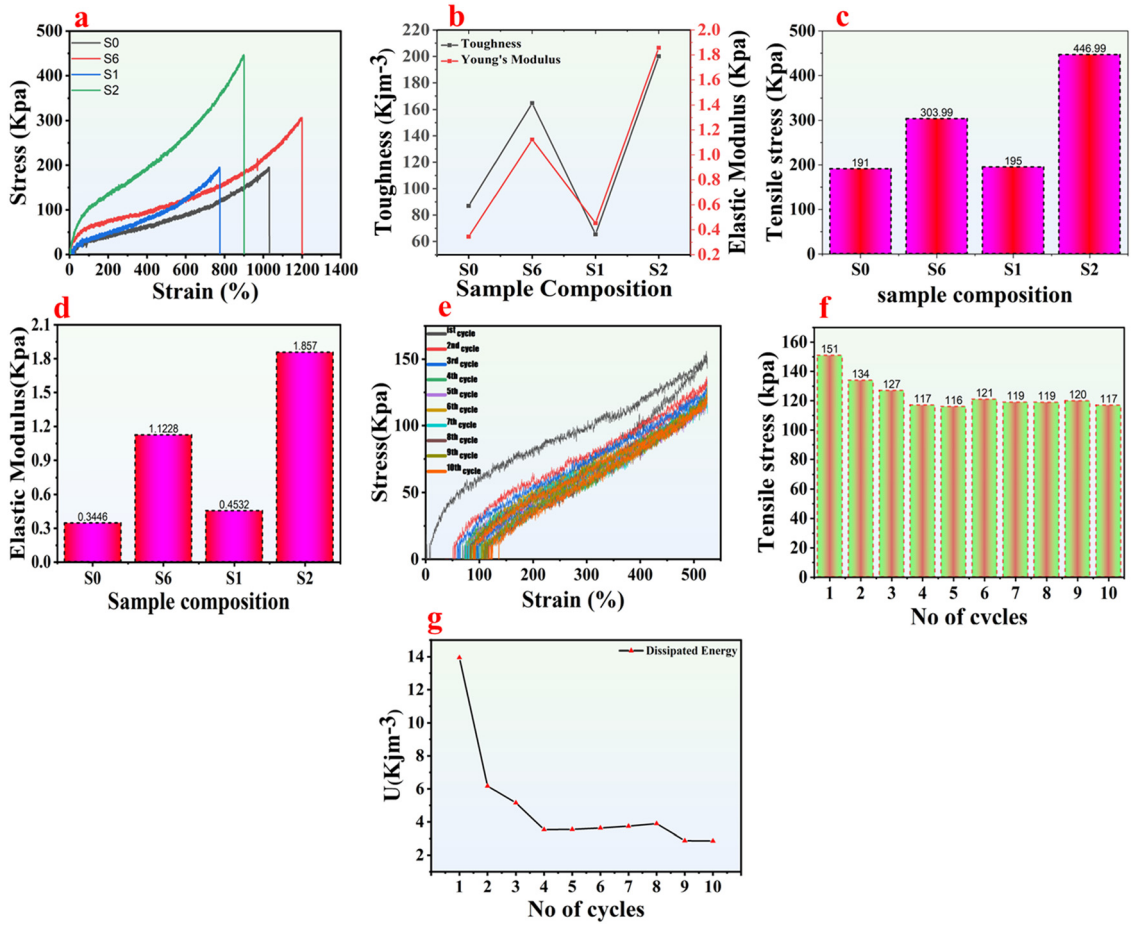


Fig. 3 Mechanical characterization of the hydrogels and organohydrogels: (a) stress verses strain curves, (b) toughness and elastic modulus, (c) tensile stress, (d) elastic modulus, (e) cyclic loading–unloading test, (f) tensile stress during multiple cycles, and (g) dissipated energy during multiple cycles.

This broader peak suggests that the samples do not crystallize simultaneously at a specific temperature but rather over a range of temperatures with maximum crystallization at the peak temperature value. Sample S6 demonstrated some antifreeze behavior, with a crystallization temperature of −5 °C, attributed to the presence of $CoCl_2{\cdot}6H_2O$. Similarly, samples S3, S4, and S5 showed peaks at −16.6 °C, −57.4 °C, and −24.4 °C, respectively, indicating their antifreeze properties. The broader peak in sample S4 suggests that 70% Gl can impart improper crystallization behavior, which is over a range of temperatures with the maximum at −57.4 °C. In contrast, there were no obvious peaks for samples S1 and S2 within the provided temperature range, indicating that these samples can function below −90 °C.

### 3.3. Mechanical characterizations

A universal testing machine (UTM) was utilized to carry out tensile and cyclic tensile tests to ensure the mechanical strength of the designed hydrogels and organohydrogels, as shown in Video S2 (ESI†). To prepare the material for testing, samples S0 and S6 (hydrogels), and S1 and S2 (organohydrogels) were cut into 50 mm length, 10 mm width, and 1.5 mm thickness before being subjected to UTM testing. The tensile performance of samples S0, S6, S1, and S2 is shown in Fig. 3a, demonstrating that sample S6 has achieved the highest mechanical strength, displaying an impressive fracture strain of up to 1200%. By comparing with samples S0 and S6, the higher increase in mechanical strength is due to the addition of Ag to the hydrogel matrix, which shows the reinforcement effect of the Ag and its successful incorporation into the hydrogel network. Fig. 3a also indicates that the replacement of the solvent from the hydrogels with Eg and Gl to form organohydrogels negatively affects the mechanical strength of the synthesized material. This decrease in elastic properties of the organohydrogels is attributed to the different swelling ratios in Eg and Gl solvent.[31]

Furthermore, the hydrogen bonding between the water molecules is disturbed by replacing water with Eg or Gl. By comparing the mechanical strength of the organohydrogels, the breaking point of sample S2 is at 900% strain, whereas that of sample S1 is at 790% strain. The greater reduction in both tensile stress and strain for S1 is attributed to the fewer active sites on Eg compared to Gl, as well as the differing swelling ratios in the solvent used. Furthermore, the existing van der Waals forces among Ag, water, and the hydrogel network is disturbed, and it could not regain its strength after replacing water with Eg.[32] Fig. 3b shows a comparative study of the toughness and elastic modulus of the synthesized materials. It can be deduced that the incorporation of the Ag into the hydrogels and then the subsequent replacement of the solvent with the Gl had a profound effect on the material toughness, and its performance increased significantly.

On the contrary, the replacement of water with Eg negatively affected the material performance in terms of toughness and elastic modulus. Similarly, Fig. 3c shows that sample S2 has the highest stiffness, which increases from 191 kPa to 447 kPa, indicating that the material displays higher resistance to deformation, showing the effect of Gl on the synthesized material. This enhancement in the material stiffness is because of the physical cross-linking of Ag and Gl due to numerous active sites on their side chain. Fig. 3d shows the Young's modulus of the material, which is highest (1.87 kPa) in the case of sample S2. Based on these studies, organohydrogel S2 was further considered for tensile cyclic loading–unloading testing to check its anti-fatigue performance. Fig. 3e shows a series of ten stretching cyclic tests, which shows that the hysteresis curves almost perfectly overlap after the 1st cycle, showing the remarkable fatigue resistance of the organohydrogel S2. This is also depicted in Fig. 3f, which suggests how the organohydrogel S2 responds to deformation forces during the ten consecutive cyclic tests. Fig. 3g indicates an energy dissipation mechanism in the organohydrogels, the primary source of which is hydrogen bonding. During the deformation process, these dynamic and reversible physical bonds, which also function as sacrificial bonds, effectively disperse mechanical stress and energy.[33]

### 3.4. Water retention capacity and environmental resilience of the organohydrogels

The improved resistance to drying of the organohydrogels is credited to the pivotal function of the Eg and Gl in inhibiting the creation of ice crystal structures at temperatures below freezing.[34,35] This inhibition establishes robust hydrogen bonds between Eg, Gl, and water ($H_2O$) molecules. The bonding between $H_2O$ molecules is further impeded by Eg and Gl molecules, disrupting hydrogen bond formation. $H_2O$ within the hydrogels can exist in three distinct states ''free water,'' ''intermediate water,'' and ''non-rotational bound water''.[32] Free water undergoes freezing at typical freezing points and readily interacts with Eg and Gl during the solvent-replacement mechanism. Intermediate water, associated with polymer chains or other chemicals within the hydrogels, freezes at temperatures lower than the standard freezing point due to its loose binding. Non-rotational bound water, also termed as unfrozen bound water, is attached to polymers or solvents through multiple hydrogen bonds. Eg and Gl can replace free water through the USRS. Additionally, free water transitions into intermediate or unfrozen bound water through interaction with Eg and Gl are facilitated by hydrogen bond formation.[8,32] Consequently, the freezing point of the organohydrogels experiences a substantial reduction owing to the significant decrease in free water content.

Herein, we have kept a small piece of samples S1, S2, S3, and S6 with known dimensions and weight in an open environment at RT, RH of 58%, and noted the weight loss in each case over 8 days and extended this duration for two months. The weight loss in the case of sample S6 was found to be 22.6%. Similarly, the weight loss was 11.3%, 8%, and 13.6% in the case of sample S1, sample S2, and sample S3, respectively. It is clear from Fig. 4a, that the sample without soaking lost its stretchability, became hard and brittle, and lost its original color after some days. Furthermore, a higher water retention capacity was noted in the case of S2 because of more hydrogen bonding

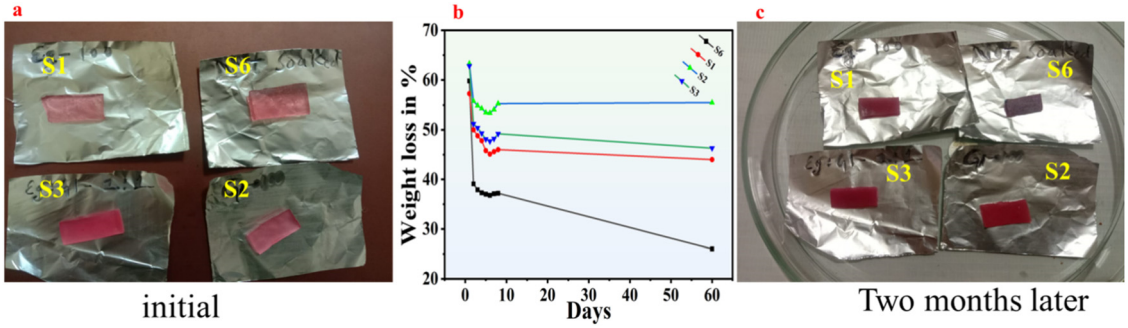


Fig. 4 Photographs and the water retention capacity of the hydrogels and organohydrogels: (a) representation of the initial condition of the samples S1, S2, S3, and S6, (b) the graphical representation of water loss over a period of two months, and (c) representation of the same mentioned samples after two months in an open environment.

capability due to the creation of numerous numbers of active sites when replaced with water. Similarly, the weight loss after the 4th day was negligible and when the samples were investigated after two months, no significant water loss was observed in the case of samples S2 and S3, showing the environmental resilience and durability of these samples, as shown in Fig. 4(b) and (c).

### 3.5. Examination of the viscoelastic properties of the organohydrogels

A rheological investigation has been carried out for both synthesized hydrogels and organohydrogels. As depicted in Fig. S3a (ESI†), there were no discernible alterations in storage modulus ($G'$) and loss modulus ($G''$) of the sample S0 and S6 hydrogels across shear rates ranging from 0.1 to 100 rad $s^{-1}$. Moreover, $G'$ consistently exceeded $G''$, suggesting the presence of a well-established cross-linked network formed by Ag within the hydrogel matrix. Fig. S3b (ESI†) illustrates the strain sweep study in the range of 0.01 to 1000 strains demonstrating that the poly(Am-*co*-LM@Ag) hydrogel retained its cross-linked network integrity and linear viscoelastic region (LVR) until the strain surpassed 19.21%. Similarly, Fig. 5a shows the frequency sweep of organohydrogels S1 and S2 ranging from 0.1 to 100 rad $s^{-1}$. There is a subsequent increase in the $G'$ and $G''$ as the angular frequency increases, showing that the materials ability to form cross-linking strengthens at higher angular frequency. Fig. 5b shows the results of the amplitude sweep study of S1 and S2. It has been concluded that the replacement of water from the hydrogel matrix with Eg or Gl can decrease the $G'$ and slightly increase the $G''$, shifting the characteristics of the designed material towards a viscous nature.[30] By comparing the $G'$ and $G''$ of the sample S6 and sample S2, the decrease found in the $G'$ was 1.94 kPa. In contrast, the increase noted in $G''$ was 4.77 kPa. Similarly, the LVR region has also been decreased to 0.1% by comparing the critical strain value from Fig. 5b and Fig. S3b (ESI†) through the relative change formula. These results suggest the successful replacement of water with Eg or Gl, also indicating their effect on the rheological properties of the hydrogels.

### 3.6. Strain sensing

Typically, conventional hydrogels experience a loss of both elasticity and electrical conductivity when subjected to subzero temperatures, primarily due to the formation of ice crystals. However, the as-prepared poly(Am-*co*-LM@Ag) organohydrogels exhibited sustained conductivity at −15 °C, showcasing remarkable resistance to freezing and consistent electrical conductivity (Fig. S4, ESI†). To investigate the relationship

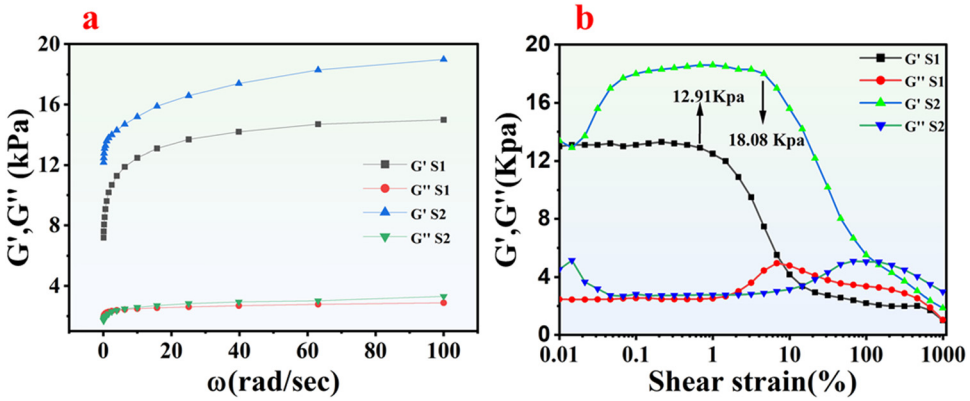


Fig. 5 The rheological investigation of the samples S1 and S2. (a) The frequency sweep test between 0.1 to 100 rad $s^{-1}$, (b) the amplitude sweep study performed for strains ranging from 0.01 to 1000% at constant frequency of 10 rad $s^{-1}$.

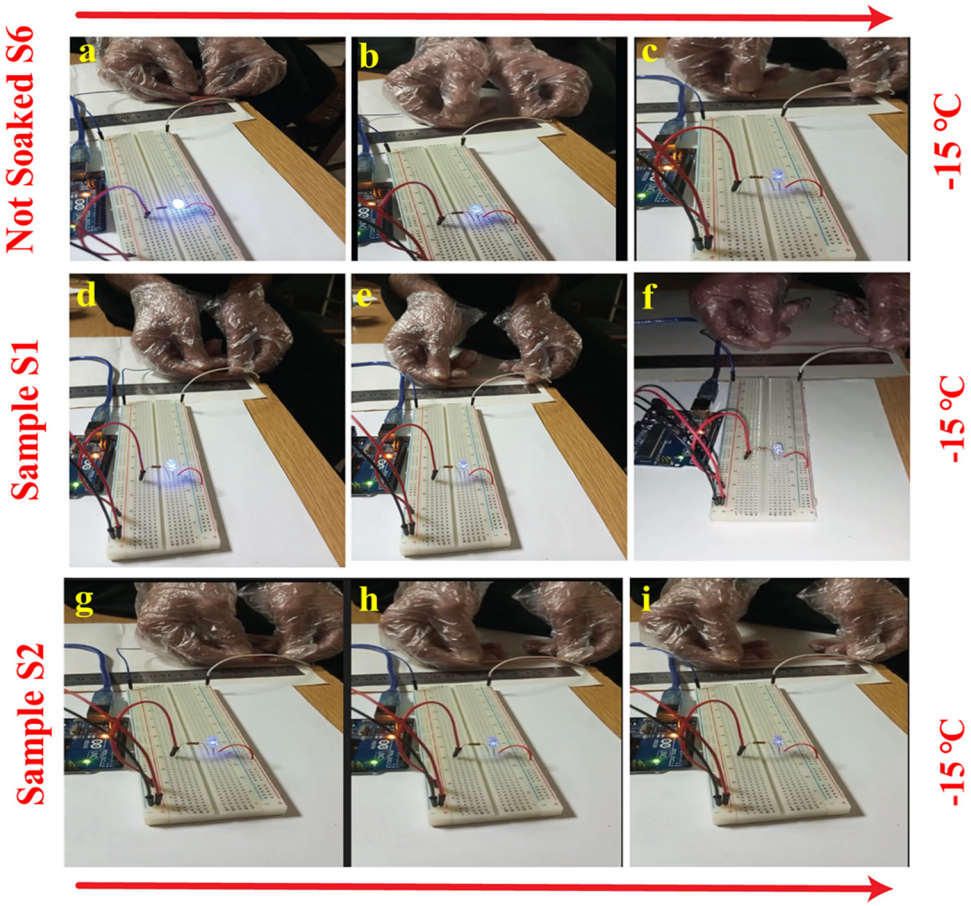


Fig. 6 Photographs showing LED response toward stretching at different strain levels at −15 °C: (a)–(c) shows the LED response of S6, (d)–(f) is the LED response of S1, and (g)–(i) is the LED response of S2.

between the current and the strain, a circuit comprising an LED light and Arduino-based project powered by 5 V DC supplied from a laptop was established. The circuit was closed with a small portion of organohydrogel by connecting it in two electrodes. The hydrogel conductivity was achieved by adding $CoCl_2{\cdot}6H_2O$ into the hydrogel matrix. The organohydrogel demonstrated a measured conductivity of 0.45 S $m^{-1}$. To check the strain sensing at a subzero temperature under normal and stretched positions, the organohydrogel was stored at −15 °C for 1 hr, and then the test was carried out; Fig. S4 (ESI†) shows the average position of the electrical strain performance.

Similarly, the strain sensing at different stretched levels for S6, S1, and S2 at −15 °C is shown in Fig. 6(a)–(i). It can be deduced that the hydrogel network facilitated the conduction of $Co^{2+}$ and $Cl^-$ ions when an electric potential is applied, allowing ions to move through the hydrogel pores, resulting in ionic conductivity. Stretching the hydrogels enlarged the ion conduction pathway, increasing resistance and reducing LED brightness, as shown in Video S3 (ESI†). Releasing the stress restored the hydrogels to its original length, intensifying LED brightness and showcasing remarkable strain sensitivity and reversibility.

Additionally, a range of strain levels were applied to the organohydrogels after storing at −15 °C, taking one reading each time and then storing again for 1 hour. We systematically performed different stretching and release cycles through autolab by performing chronoamperometry at an applied potential of 1 V. Fig. 7(a) and (b) indicate that as the percent strain rises from 1% to 50% and 10% to 600%, resistance concurrently increases. This trend suggests that the pores within the hydrogel constrict as their length increases, making the movement of ions more challenging. This trend also shows the excellent sensitivity of the fabricated organohydrogels towards both small and large strains (1% and 600%), respectively. The response time of the as-fabricated hydrogels is found by conducting rapid stretching and subsequent relaxation experiments at a 400% strain level. The results revealed response and recovery times of 0.1 seconds (100 milliseconds) and 0.08 seconds (80 milliseconds), respectively (Fig. 7c), which surpasses those of other hydrogels and organohydrogels previously synthesized.[36,37] This swift reaction to strain indicates that the synthesized hydrogels exhibits robustness and retain elastic energy efficiently even under low dissipation.

Consequently, it can swiftly rebound when subjected to stretching or compression. To further elucidate the stability of the organohydrogels, multiple cycles and slow-fast stretching were performed. Fig. 7d shows the organohydrogels response towards multiple cycles, during which 200 cycles were

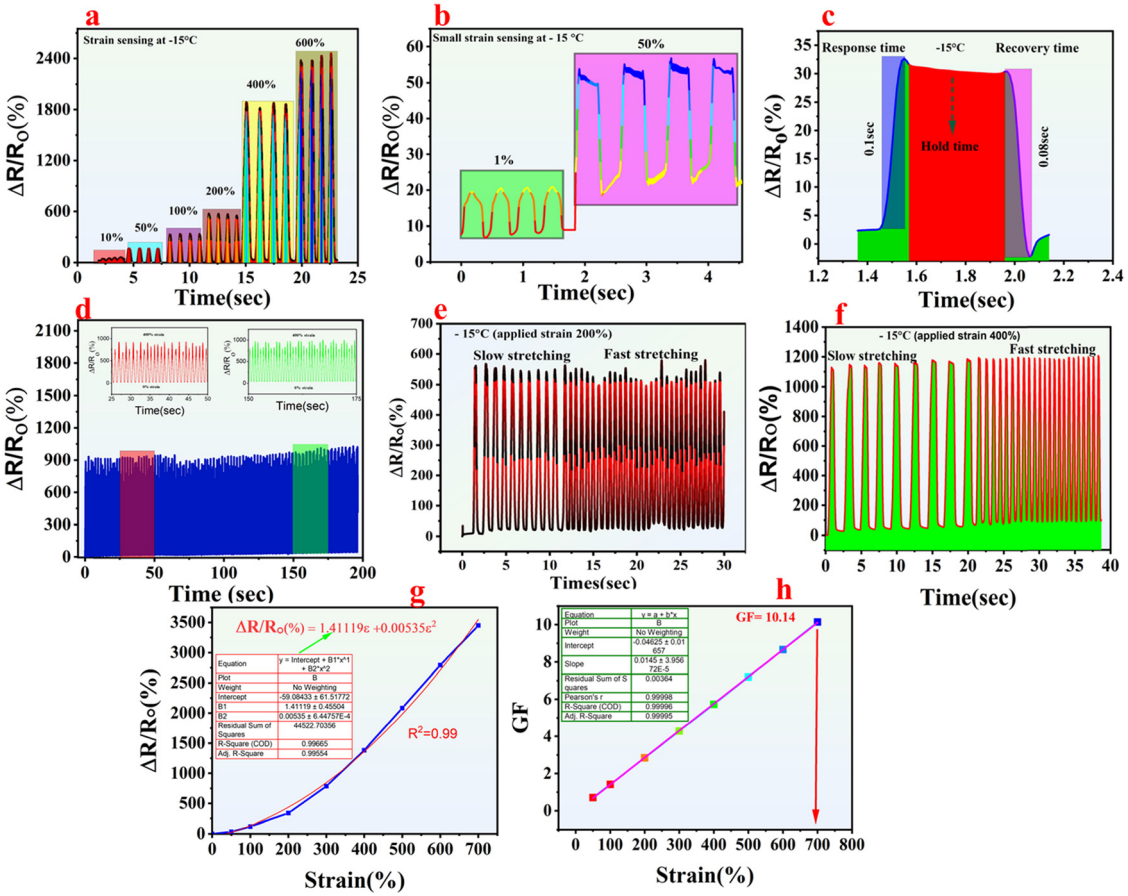


Fig. 7 (a) and (b) Strain sensitivity, (c) response and recovery time, (d) multiple cycles test, (e) and (f) slow-fast stretching of the organohydrogels, (g) polynomial fit percent relative resistance, and (h) obtained gauge factor in terms of linear fit.

performed by continuously stretching and relaxing the organohydrogels for 200 seconds at 400% strain. There is no significant current drop observed, which shows the remarkable antifatigue resistance of the as-fabricated organohydrogels. The material stability was further confirmed by taking 500 cycles at 200% strain, and again no significant current drop was observed (Fig. S5, ESI†). In the same way, slow fast stretching was performed at different strain levels as shown in Fig. 7(e) and (f) −15 °C. This also suggests the stability and reproducibility of the material as the peaks generated are the same every time.

Furthermore, the strain sensitivity was also analyzed using the gauge factor (GF), a crucial quantitative measure for assessing material strain sensitivity. GF is determined by the formula previously used in the literature as $(\Delta R)/(R^{\circ})/\varepsilon$. Fig. 7(g) and (h) illustrate that the organohydrogels exhibited an outstanding linear relationship between the relative change in resistance $(\Delta R)/(R_0)$ and strain.

The linearity, as indicated by the correlation coefficient ($R^2$), achieved a value of 0.99. The relative resistance (RR) was determined using $\Delta R/R_0$ (%) = $1.41119\varepsilon + 0.00535\varepsilon^2$ and then a linear fit was applied to calculate the GF, as shown in Fig. 7g.

Fig. 7h indicates that as strain increases, the GF enhances and at an applied strain of 700%, the calculated GF value obtained was 10.14, which exceeds those reported in previous studies underscoring the compassionate nature of the organohydrogels.[38,39] All these findings suggest that the as-fabricated organohydrogel is a good fit for cyclic activities, highlighting its superior strain sensitivity under subzero temperatures. The key parameters of the current research compared with the most recent one of the same type are presented in Table S1 (ESI†). It can be deduced that although some of the synthesized materials have amazing sensitivity and conductivity, their working range is limited to RT. Some of them can work under a wide range of temperatures, but their sensitivity and stretchability are reduced.

### 3.7. Wearable sensors designed to track and analyze the motions of muscles and joints, enhancing human–machine interaction

As human–machine interaction (HMI) becomes increasingly integrated into our daily routines, there is a growing demand for more convenient and intelligent interfaces. Traditional HMI devices often utilize rigid materials that suffer from fragility and inflexibility.[40,41] The hydrogels, renowned for their robust mechanical properties, exceptional biocompatibility, and heightened sensitivity, have emerged as promising candidates for HMI systems, garnering significant attention from researchers.[42]

However, the prevalent issue with hydrogels is their susceptibility to drying and freezing, particularly in low-temperature environments, leading to inactivation. Hence, there is a pressing need to innovate and develop a new breed of antifreeze gel materials capable of withstanding harsh cold conditions and resisting evaporation.[43] Herein, the synthesized organohydrogels have remarkable anti-freezing and anti-drying capabilities, heightened strain sensitivity, good electrical stability, and robust mechanical properties. All these properties make the designed organohydrogels suitable for flexible wearable electronics, wearable robotics, and human motion detection. To perform some human motion tests, a circuit was devised by integrating an organohydrogel strip with an automated laboratory system. The organohydrogel strip, once connected, was affixed to various mobile joints on the body using scotch tape. This setup enabled detection at both singular and varied angles for comprehensive testing. Fig. 8a shows the finger bending response at a single angle. As the finger flexed to a specific degree, the organohydrogels underwent stretching, causing a temporary decrease in the current. Upon the finger returning to its original position, the current drop normalized accordingly.[44] Similarly, Fig. 8b shows the response of the organohydrogels to the finger movement across various angles at subzero temperature. It was observed that with an increase in the finger angle, there is a corresponding increase in the percent relative resistance. Upon the finger restoration to its initial orientation, the percentage relative resistance reverted to its baseline level.

In the same way, Fig. 8c shows the response of organohydrogels to the elbow movement at various angles. This shows that as the elbow is bent for the 2nd time to the same angle, the current drop is similar which confirms the stability and reproducibility of the organohydrogels. Fig. 8d shows the response of the organohydrogels towards elbow movements at one specific angle. The organohydrogel sensitivity was further illustrated by affixing it onto the arm muscles. This resulted in distinct current–time peaks during muscle contraction and relaxation, as depicted in Fig. 8e. The organohydrogel response during handshaking can be shown in Fig. 8f, which shows that as the volunteers shake hands, the current drop occurs for a short period and gets normalized as the volunteers let go of each other's hands.

Furthermore, the meticulously designed organohydrogels demonstrates precision by detecting human voice, coughing signals, minute pressure through pen touch, and pressing keys on a keyboard even at subzero temperatures. As depicted in Fig. 9a, each time the volunteer coughs, the organohydrogels deliver a distinct signal, showcasing its reliable performance. Similarly, when the organohydrogels were affixed to the volunteer's vocal cords, it consistently detected the word "antifreezing" with a specific signal upon pronunciation, as shown in Fig. 9b. The organohydrogel's ability to detect even the slightest pressure is demonstrated in Video S4 (ESI†). When the volunteer lightly touches the organohydrogel with a pen tip, a small signal is generated, affirming that the current drop occurs even with a minuscule touch to the organohydrogel (Fig. 9c). To ensure the reliability of our findings, the organohydrogel was rigorously tested. In one such test, the organohydrogel was affixed to the volunteer's forefinger, and their response to pressing the keyboard keys was analyzed. Fig. 9d presents the response when the volunteer presses the space button on the keyboard. These tests were repeated with five different segments of the same sample of S2, with each segment stored at −15 °C for 1 hour after each test, to mimic

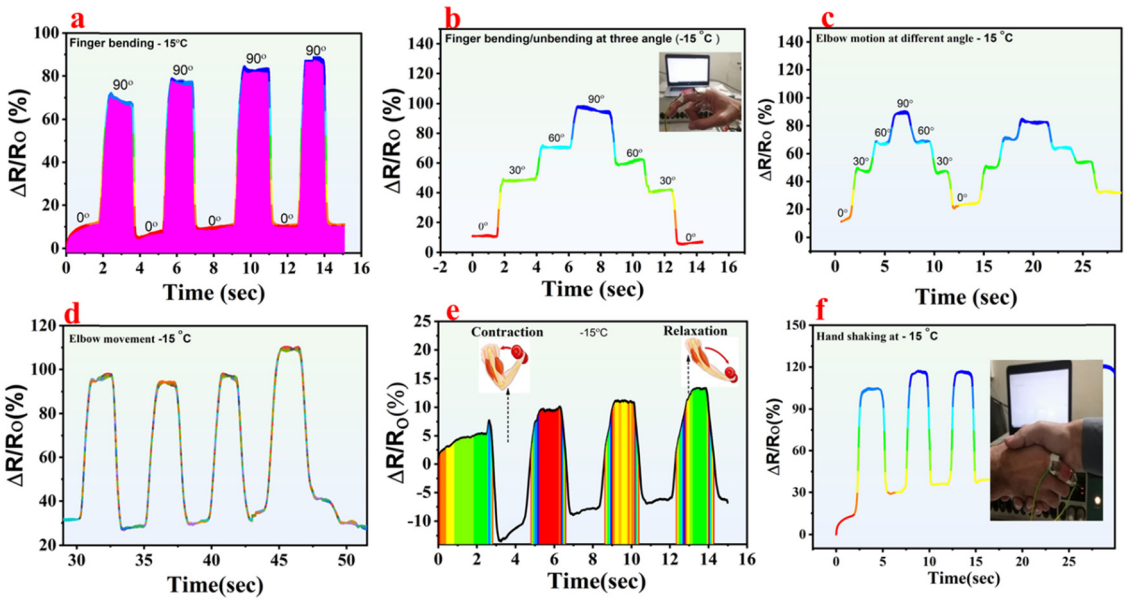


Fig. 8 Human motion detection: (a) finger bending and unbending at one angle, (b) finger bending and unbending at various angles, (c) elbow bending and unbending at different angles, (d) elbow bending and unbending at one angle, (e) the muscle contraction and relaxation response, and (f) the response of the organohydrogels towards hand shaking of volunteers.

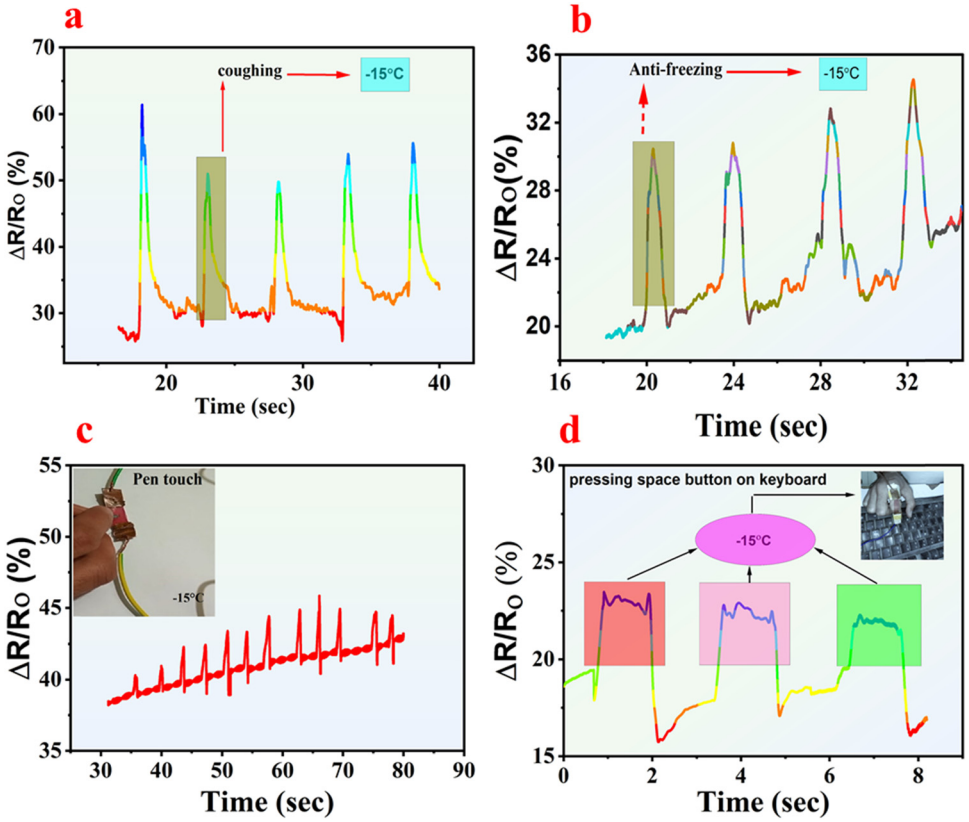


Fig. 9 Organohydrogels for human motion detection, (a) response to the coughing of a volunteer, (b) voice detection response when the volunteer pronounces it, (c) pressure response towards a small pen touch, and (d) response to pressing of a keyboard button.

real-world conditions and verify the organohydrogel's consistent performance.

## 4. Conclusion

A straightforward technique was successfully devised to create conductive organohydrogels for enhanced applications in strain sensing, human motion detection, and soft robotics. Thanks to the strong hydrogen bonding of Eg and Gl with water and the poly(Am-*co*-LM@Ag) hydrogel network, organohydrogels with exceptional stretchability, durability, strain sensing, and anti-freezing capabilities are produced. Specifically, the strain sensor displays high mechanical performance of 850% strain within the temperature range of −15 °C to 25 °C. The as-fabricated strain sensor also shows a stable response toward the smallest pressure applied with a pen tip. Additionally, it can detect multilevel strain from small (1%) to large (600%) with high sensitivity GF = 10.14. Due to its high sensitivity, compatibility, and human skin-like characteristics this strain sensor can be comfortably attached to the human body to detect various motions across a wide temperature range. It reliably monitors different movements, like finger typing, and hand shaking, muscle contraction and relaxation. Despite focusing on just one type of hydrogel, this straightforward and versatile solvent-replacement approach could be used to improve the properties of various other hydrogels.

## Data availability

This work is original research, with primary research/new data available in the figures.

## Conflicts of interest

The authors declare that no conflict of interest exists.

## Acknowledgements

The authors extend their appreciation to the researchers supporting project (RSP2024R171), King Saud University, Riyadh, Saudi Arabia for financial support.

## References

1 H. Yang, X. Yao, Z. Zheng, L. Gong, L. Yuan, Y. Yuan and Y. Liu, Highly sensitive and stretchable graphene-silicone rubber composites for strain sensing, *Compos. Sci. Technol.*, 2018, **167**, 371–378.
2 H. Y. Chen, Z. Y. Chen, M. Mao, Y. Y. Wu, F. Yang, L. X. Gong, L. Zhao, C. F. Cao, P. Song and J. F. Gao, Self-adhesive polydimethylsiloxane foam materials decorated with MXene/cellulose nanofiber interconnected network for versatile functionalities, *Adv. Funct. Mater.*, 2023, **33**(48), 2304927.

3 J. H. Lee, S. H. Kim, J. S. Heo, J. Y. Kwak, C. W. Park, I. Kim, M. Lee, H. H. Park, Y. H. Kim and S. J. Lee, Heterogeneous structure omnidirectional strain sensor arrays with cognitively learned neural networks, *Adv. Mater.*, 2023, **35**(13), 2208184.
4 M. Manti, V. Cacucciolo and M. Cianchetti, Stiffening in soft robotics: a review of the state of the art, *IEEE Rob. Automation Mag.*, 2016, **23**(3), 93–106.
5 C. Laschi, B. Mazzolai and M. Cianchetti, Soft robotics: technologies and systems pushing the boundaries of robot abilities, *Sci. Rob.*, 2016, **1**(1), eaah3690.
6 T. da Veiga, J. H. Chandler, P. Lloyd, G. Pittiglio, N. J. Wilkinson, A. K. Hoshiar, R. A. Harris and P. Valdastri, Challenges of continuum robots in clinical context: a review, *Prog. Biomed. Eng.*, 2020, **2**(3), 032003.
7 Y. Zhou, B. He, Z. Yan, Y. Shang, Q. Wang and Z. Wang, Touch locating and stretch sensing studies of conductive hydrogels with applications to soft robots, *Sensors*, 2018, **18**(2), 569.
8 J. Wu, Z. Wu, X. Lu, S. Han, B.-R. Yang, X. Gui, K. Tao, J. Miao and C. Liu, Ultrastretchable and stable strain sensors based on antifreezing and self-healing ionic organohydrogels for human motion monitoring, *ACS Appl. Mater. Interfaces*, 2019, **11**(9), 9405–9414.
9 Y. Chen, Y. Zhang, H. Li, J. Shen, F. Zhang, J. He, J. Lin, B. Wang, S. Niu and Z. Han, Bioinspired hydrogel actuator for soft robotics: opportunity and challenges, *Nano Today*, 2023, **49**, 101764.
10 Q.-Y. Ni, X.-F. He, J.-L. Zhou, Y.-Q. Yang, Z.-F. Zeng, P.-F. Mao, Y.-H. Luo, J.-M. Xu, B. Jiang and Q. Wu, Mechanical tough and stretchable quaternized cellulose nanofibrils/MXene conductive hydrogel for flexible strain sensor with multi-scale monitoring, *J. Mater. Sci. Technol.*, 2024, **191**, 181–191.
11 S. Yazdani, M. Khan, A. Shahzad, L. A. Shah and D. Ye, Ionic conductive hydrogels formed through hydrophobic association for flexible strain sensing, *Sens. Actuators, A*, 2023, **350**, 114148.
12 R. Ullah, L. A. Shah, M. Khan and L. Ara, Guar gum reinforced conductive hydrogel for strain sensing and electronic devices, *Int. J. Biol. Macromol.*, 2023, **246**, 125666.
13 Q. Rong, W. Lei, L. Chen, Y. Yin, J. Zhou and M. Liu, Antifreezing, conductive self-healing organohydrogels with stable strain-sensitivity at subzero temperatures, *Angew. Chem., Int. Ed.*, 2017, **56**(45), 14159–14163.
14 X. P. Morelle, W. R. Illeperuma, K. Tian, R. Bai, Z. Suo and J. J. Vlassak, Highly stretchable and tough hydrogels below water freezing temperature, *Adv. Mater.*, 2018, **30**(35), 1801541.
15 C. Keplinger, J.-Y. Sun, C. C. Foo, P. Rothemund, G. M. Whitesides and Z. Suo, Stretchable, transparent, ionic conductors, *Science*, 2013, **341**(6149), 984–987.
16 X. Liu, Q. Zhang and G. Gao, Solvent-resistant and non-swellable hydrogel conductor toward mechanical perception in diverse liquid media, *ACS Nano*, 2020, **14**(10), 13709–13717.
17 B. Li, Y. Zhang, C. Wu, B. Guo and Z. Luo, Fabrication of mechanically tough and self-recoverable nanocomposite hydrogels from polyacrylamide grafted cellulose nanocrystal and poly(acrylic acid), *Carbohydr. Polym.*, 2018, **198**, 1–8.
18 D. Zhou, F. Chen, S. Handschuh-Wang, T. Gan, X. Zhou and X. Zhou, Biomimetic Extreme-Temperature-and Environment-Adaptable Hydrogels, *ChemPhysChem*, 2019, **20**(17), 2139–2154.
19 Y.-Y. Lee, H.-Y. Kang, S. H. Gwon, G. M. Choi, S.-M. Lim, J.-Y. Sun, Y.-C. Joo and A. Strain-Insensitive, Stretchable Electronic Conductor: PEDOT:PSS/Acrylamide Organogels, *Adv. Mater.*, 2015, **28**(8), 1636–1643.
20 L. Han, K. Liu, M. Wang, K. Wang, L. Fang, H. Chen, J. Zhou and X. Lu, Mussel-inspired adhesive and conductive hydrogel with long-lasting moisture and extreme temperature tolerance, *Adv. Funct. Mater.*, 2018, **28**(3), 1704195.
21 H. Yue, Y. Zhao, X. Ma and J. Gong, Ethylene glycol: properties, synthesis, and applications, *Chem. Soc. Rev.*, 2012, **41**(11), 4218–4244.
22 W. Wang, S. Ummartyotin and R. Narain, Advances and challenges on hydrogels for wound dressing, *Curr. Opin. Biomed. Eng.*, 2023, 100443.
23 M. Khan, T. U. Rahman, M. Sher, L. A. Shah, H. Md Akil, J. Fu and H.-M. Yoo, Flexible Ionic Conductive Hydrogels with Wrinkled Texture for Flexible Strain Transducer with Language Identifying Diversity, *Chem. Mater.*, 2024, **36**(9), 4703–4713.
24 M. Sher, L. A. Shah, L. Ara, R. Ullah, M. Khan, H.-M. Yoo and J. Fu, Xanthan gum toughen ionically conductive hydrogels for flexible and artificial epidermis sensors with multifunctionality and self-healability, *Sens. Actuators, A*, 2024, 115199.
25 M. Khan, L. A. Shah, T. U. Rahman, H.-M. Yoo, D. Ye and J. Vacharasin, Cellulose nanocrystals boosted hydrophobic association in dual network polymer hydrogels as advanced flexible strain sensor for human motion detection, *J. Mech. Behav. Biomed. Mater.*, 2023, **138**, 105610.
26 L. Ara, M. Khan, R. Ullah and L. A. Shah, Hydrophobically associated ionic conductive hydrogels as strain, pressure, and an electronic sensor for human motions detection, *Sens. Actuators, A*, 2023, **362**, 114618.
27 Y. Ye, Z. Wan, P. Gunawardane, Q. Hua, S. Wang, J. Zhu, M. Chiao, S. Renneckar, O. J. Rojas and F. Jiang, Ultra-Stretchable and Environmentally Resilient Hydrogels Via Sugaring-Out Strategy for Soft Robotics Sensing, *Adv. Funct. Mater.*, 2024, 2315184.
28 G. Akay, A. Hassan-Raeisi, D. C. Tuncaboylu, N. Orakdogen, S. Abdurrahmanoglu, W. Oppermann and O. Okay, Self-healing hydrogels formed in catanionic surfactant solutions, *Soft Matter*, 2013, **9**(7), 2254–2261.
29 M. Sasaki, B. C. Karikkineth, K. Nagamine, H. Kaji, K. Torimitsu and M. Nishizawa, Highly conductive stretchable and biocompatible electrode–hydrogel hybrids for advanced tissue engineering, *Adv. Healthcare Mater.*, 2014, **3**(11), 1919–1927.
30 C. Li, X. Deng and X. Zhou, Synthesis antifreezing and antidehydration organohydrogels: one-step in situ gelling versus two-step solvent displacement, *Polymers*, 2020, **12**(11), 2670.
31 R. Rodríguez-Rodríguez, H. Espinosa-Andrews, C. Velasquillo-Martínez and Z. Y. García-Carvajal, Composite hydrogels

based on gelatin, chitosan and polyvinyl alcohol to biomedical applications: a review, *Int. J. Polym. Mater. Polym. Biomater.*, 2020, **69**(1), 1–20.

32 J. Wu, Z. Wu, Y. Wei, H. Ding, W. Huang, X. Gui, W. Shi, Y. Shen, K. Tao and X. Xie, Ultrasensitive and stretchable temperature sensors based on thermally stable and self-healing organohydrogels, *ACS Appl. Mater. Interfaces*, 2020, **12**(16), 19069–19079.

33 L. Zhou, Y. Li, J. Xiao, S.-W. Chen, Q. Tu, M.-S. Yuan and J. Wang, Liquid metal-doped conductive hydrogel for construction of multifunctional sensors, *Anal. Chem.*, 2023, **95**(7), 3811–3820.

34 L. Sun, Z. Zhu and D.-W. Sun, Regulating ice formation for enhancing frozen food quality: materials, mechanisms and challenges, *Trends Food Sci. Technol.*, 2023, **139**, 104116.

35 C. Shen, E. F. Julius, T. J. Tyree, D. W. Moreau, H. Atakisi and R. E. Thorne, Thermal contraction of aqueous glycerol and ethylene glycol solutions for optimized protein-crystal cryoprotection, *Acta Crystallogr., Sect. D: Struct. Biol.*, 2016, **72**(6), 742–752.

36 X. Sun, Z. Qin, L. Ye, H. Zhang, Q. Yu, X. Wu, J. Li and F. Yao, Carbon nanotubes reinforced hydrogel as flexible strain sensor with high stretchability and mechanically toughness, *Chem. Eng. J.*, 2020, **382**, 122832.

37 M. Khan, L. A. Shah, H. Hifsa, H.-M. Yoo and D.-J. Kwon, Bimetallic-MOF Tunable Conductive Hydrogels to Unleash High Stretchability and Sensitivity for Highly Responsive Flexible Sensors and Artificial Skin Applications, *ACS Appl. Polym. Mater.*, 2024, **6**(12), 7288–7300.

38 H. Zhang, W. Niu and S. Zhang, Extremely stretchable, stable, and durable strain sensors based on double-network organogels, *ACS Appl. Mater. Interfaces*, 2018, **10**(38), 32640–32648.

39 C.-Z. Hang, X.-F. Zhao, S.-Y. Xi, Y.-H. Shang, K.-P. Yuan, F. Yang, Q.-G. Wang, J.-C. Wang, D. W. Zhang and H.-L. Lu, Highly stretchable and self-healing strain sensors for motion detection in wireless human–machine interface, *Nano Energy*, 2020, **76**, 105064.

40 R. Yin, D. Wang, S. Zhao, Z. Lou and G. Shen, Wearable sensors-enabled human–machine interaction systems: from design to application, *Adv. Funct. Mater.*, 2021, **31**(11), 2008936.

41 Y. Wang, P. Zhu, M. Tan, M. Niu, S. Liang and Y. Mao, Recent Advances in Hydrogel-Based Self-Powered Artificial Skins for Human–Machine Interfaces, *Adv. Intelligent Syst.*, 2023, **5**(9), 2300162.

42 W. Heng, S. Solomon and W. Gao, Flexible electronics and devices as human–machine interfaces for medical robotics, *Adv. Mater.*, 2022, **34**(16), 2107902.

43 Z. Fu, H. Liu, Q. Lyu, J. Dai, C. Ji and Y. Tian, Anti-freeze hydrogel-based sensors for intelligent wearable human–machine interaction, *Chem. Eng. J.*, 2024, 148526.

44 G. Ge, Y. Zhang, J. Shao, W. Wang, W. Si, W. Huang and X. Dong, Stretchable, transparent, and self-patterned hydrogel-based pressure sensor for human motions detection, *Adv. Funct. Mater.*, 2018, **28**(32), 1802576.